3. P. T. Todorov *et al.*, *Cancer Res.* **58**, 2353 (1998); K. Hirai, H. J. Hussey, M. D. Barber, S. A. Price, M. J. Tisdale, *ibid.*, p. 2359.
4. Protein sequences: Human ZAG [T. Araki *et al.*, *Proc. Natl. Acad. Sci. U.S.A.* **85**, 679 (1988)]; mouse ZAG [H. Ueyama, H. Naitoh, I. Ohkubo, *J. Biochem.* **116**, 677 (1994)]; rat ZAG [A. Fueyo, J. A. Uría, J. P. Freije, C. López-Otín, *Gene* **145**, 245 (1994)]. Human class I MHC sequences [P. J. Bjorkman and P. Parham, *Annu. Rev. Biochem.* **59**, 253 (1990)]; MHC homolog sequences, SWISS-PROT [A. Bairoch and R. Apweiler, *Nucleic Acids Res.* **26**, 38 (1998)]. Sequence identities: ZAG and HLA-A2, 36%; ZAG and FcRn, 27%; ZAG and mouse CD1d, 23%; ZAG and HFE, 36%; ZAG and MIC-A, 29%.
5. D. R. Madden, *Annu. Rev. Immunol.* **13**, 587 (1995).
6. E. M. Beckman *et al.*, *Nature* **372**, 691 (1994); A. R. Castaño *et al.*, *Science* **269**, 223 (1995).
7. R. P. Junghans, *Immunol. Res.* **16**, 29 (1997); V. Ghetie and E. S. Ward, *Immunol. Today* **18**, 592 (1997); N. E. Simister, E. J. Israel, J. C. Ahouse, C. M. Story, *Biochem. Soc. Trans.* **25**, 481 (1997).
8. J. N. Feder *et al.*, *Nature Genet.* **13**, 399 (1996); J. N. Feder *et al.*, *Proc. Natl. Acad. Sci. U.S.A.* **95**, 1472 (1998).
9. L. M. Sánchez, C. López-Otín, P. J. Bjorkman, *Proc. Natl. Acad. Sci. U.S.A.* **94**, 4626 (1997). In thermal denaturation studies, ZAG denatures with a transition midpoint of 65°C, compared to 57°C for the peptide-filled class I molecule H-2K^d and 45°C for empty K^d [M. L. Fahnestock, I. Tamir, L. Narhi, P. J. Bjorkman, *Science* **258**, 1658 (1992)].
10. V. Groh *et al.*, *Proc. Natl. Acad. Sci. U.S.A.* **93**, 12445 (1996). The crystal structure of MIC-A reveals a major rearrangement in domain organization compared to the structures of class I molecules and ZAG. The MIC-A α1-α2 platform is displaced from its α3 domain by 113.5° compared to class I molecules. As a result, the MIC-A α1-α2 platform makes no contact with its α3 domain [P. Li, S. T. Willie, S. Bauer, D. L. Morris, T. Spies, R. K. Strong, personal communication].
11. Protein structures: HLA-A2 [Protein Data Bank (PDB) code 2CLR] [E. J. Collins, D. N. Garboczi, D. C. Wiley, *Nature* **371**, 626 (1994)]; Mouse CD1 (PDB code 1CD1) [Z.-H. Zeng *et al.*, *Science* **277**, 339 (1997)]; Rat FcRn (PDB code 3FRU) [W. P. Burmeister, L. N. Gastinel, N. E. Simister, M. L. Blum, P. J. Bjorkman, *Nature* **372**, 336 (1994)]; Human HFE (PDB code 1A6Z) [J. A. Lebrón *et al.*, *Cell* **93**, 111 (1998)]. Molecular surface areas buried by interaction were calculated with X-PLOR [A. T. Brünger, *X-PLOR. Version 3.1: A System for X-ray and NMR* (Yale Univ. Press, New Haven, CT, 1992)] with a 1.4 Å radius. Identification of pocket residues and calculation of groove surface areas were done based upon earlier analyses of human and mouse class I structures [M. A. Saper, P. J. Bjorkman, D. C. Wiley, *J. Mol. Biol.* **219**, 277 (1991); M. Matsumura, D. H. Fremont, P. A. Peterson, I. A. Wilson, *Science* **257**, 927 (1992)] as described in the CD1 (Z.-H. Zeng *et al.*) and HFE (J. A. Lebrón *et al.*) structure papers. Cut away molecular surfaces of grooves (Fig. 3B) were generated as described in the CD1 structure paper.
12. S. Shibata and K. Miura, *Nephron* **31**, 170 (1982).
13. Structure determination and refinement: HKL [Z. Otwinowski and W. Minor, *Methods Enzymol.* **276**, 307 (1997)]. SHARP [E. De La Fortelle and G. Bricogne, *ibid.*, p. 472]. Solomon [J. P. Abrahams and A. G. W. Leslie, *Acta Crystallogr. D* **52**, 30 (1996)]. CCP4 programs [CCP4: Collaborative Computational Project No. 4, Daresbury, UK, *Acta Crystallogr. D* **50**, 760 (1994)]. O [T. A. Jones and M. Kjeldgaard, *Methods Enzymol.* **277**, 173 (1997)]. R_{free} [A. T. Brünger, *Nature* **355**, 472 (1992)]. The Native II data set (Table 1) was used for refinement. After rigid-body refinement of eight domains in the asymmetric unit (α1-α2 and α3 for each of four ZAG molecules) using CNS [A. T. Brünger *et al.*, *Acta Crystallogr. D* **54**, 905 (1998)], the four molecules were subjected to restrained NCS torsion-angle refinement using the maximum likelihood target function. Tight NCS restraints (300 kcal/mol·Å^2) were applied to all regions except for flexible loops and residues involved in lattice contacts. Intermediate rounds of model building and refinement included the calculation of SIGMAA-weighted [R. J. Read, *Acta Crystallogr. A* **42**, 140 (1986)] simulated annealing omit maps [A. Hodel, S.-H. Kim, A. T. Brünger, *Acta Crystallogr. A* **48**, 851 (1992)]. Final rounds of rebuilding and refinement included tightly restrained individual atomic temperature factor refinement (temperature factor rms deviation for bonded main chain and side chain atoms is 5.7 and 8.8 Å^2, respectively). The model consists of residues 5 through 277 (average *B*: 48 Å^2) with nine carbohydrate residues (average *B*: 61 Å^2) for molecule 1, residues 5 through 278 (average *B*: 56 Å^2) with 11 carbohydrate residues (average *B*: 80 Å^2) for molecule 2, residues 6 through 278 (average *B*: 57 Å^2) with four carbohydrate residues (average *B*: 107 Å^2) for molecule 3, and residues 6 through 249 and 258 through 276 (average *B*: 62 Å^2) with five carbohydrate residues (average *B*: 90 Å^2) for molecule 4 (Wilson B = 64 Å^2). Excluding regions that deviate from the NCS, the domains in the NCS-related ZAG monomers are very similar (<0.04 Å rms deviation for Cα atoms). Ramachandran plot statistics (Table 1) are as defined by G. J. Kleywegt and T. A. Jones [*Structure* **4**, 1395 (1996)].
14. Extensive carbohydrate density is found at Asn^{239} (nine ordered carbohydrate residues in molecule 2) and to a much lesser extent at Asn^{89} and Asn^{108} in all four ZAG molecules (Fig. 1) (*13*). Crystal structures of glycoproteins rarely show more than three ordered carbohydrate residues at each glycosylation site [D. E. Vaughn and P. J. Bjorkman, *Structure* **6**, 63 (1998)]. The Asn in the fourth potential N-linked glycosylation site (Asn^{92}) does not show density corresponding to carbohydrate. The bond between Asn^{92} and Gly^{93} can be cleaved by hydroxylamine, confirming that Asn^{92} is not glycosylated (*18*).
15. M. Takagaki *et al.*, *Biochem. Biophys. Res. Commun.* **201**, 1339 (1994); O. Ogikubo *et al.*, *ibid.* **252**, 257 (1998); M. Pfaff, in *Integrin-Ligand Interaction*, J. A. Eble and K. Kühn, Eds. (Chapman & Hall, New York, 1997), pp. 101–121.
16. V. A. Tysoe-Calnon, J. E. Grundy, S. J. Perkins, *Biochem. J.* **277**, 359 (1991); D. Lancet, P. Parham, J. L. Strominger, *Proc. Natl. Acad. Sci. U.S.A.* **76**, 3844 (1979); A. Bauer *et al.*, *Eur. J. Immunol.* **27**, 1366 (1997).
17. Structural features that prevent ZAG from binding β_2M include the following residues, which clash with β_2M when it is positioned on the ZAG structure either by interacting with α3 or with α1-α2: Ile^{13}, Thr^{15}, Leu^{30}, Arg^{40}, Gln^{98}, Tyr^{118}, Lys^{122}, Val^{234}, His^{236}, Trp^{245}.
18. L. M. Sánchez and P. J. Bjorkman, unpublished results.
19. G. F. Gao *et al.*, *Nature* **387**, 630 (1997).
20. D. N. Garboczi *et al.*, *ibid.* **384**, 134 (1996); K. C. Garcia *et al.*, *Science* **274**, 209 (1996); Y. H. Ding *et al.*, *Immunity* **8**, 403 (1998); K. C. Garcia *et al.*, *Science* **279**, 1166 (1998).
21. Superpositions based on Cα atoms in the platform β strands reveal that the ZAG platform is more similar to classical class I MHC molecules than to any of the class I homologs [rms deviations for superpositions of platforms: ZAG and HLA-A2, 1.3 Å (147 Cα atoms); ZAG and CD1, 1.1 Å (86 Cα atoms); ZAG and FcRn 1.0 Å (88 Cα atoms); ZAG and HFE 1.0 Å (115 Cα atoms)].
22. L. M. Sánchez, A. J. Chirino, P. J. Bjorkman, G. Hathaway, P. G. Green, K. Faull, unpublished results.
23. Figures 1, 2A (right), 2B, 3A, and 3C were made using MOLSCRIPT [P. J. Kraulis, *J. Appl. Crystallogr.* **24**, 946 (1991)] and RASTER-3D [E. A. Merritt and M. E. P. Murphy, *Acta Crystallogr. D.* **50**, 869 (1994)]. Electrostatic calculations were done and Figs. 2A (left) and 3B were made using GRASP [A. Nicholls, R. Bharadwaj, B. Honig, *Biophys. J.* **64**, A166 (1993)].
24. ZAG, CD1, HFE, and FcRn contain prolines within their α2 domain helices at a position corresponding to Val^{165} in classical class I MHC molecules (*4*). The FcRn and CD1 helices are kinked at a position near their proline residues, whereas the ZAG and HFE helices are similar to the α2 domain helices of class I molecules (*11*). Substitution of Val^{165} for proline in the mouse class I molecule H-2D^d did not interfere with binding and presentation of peptides to T cells, suggesting that no major structural rearrangements occurred [D. Plaksin, K. Polakova, M. G. Mage, D. H. Margulies, *J. Immunol.* **159**, 4408 (1997)].

25. We thank G. Hathaway, P. G. Green, and K. Faull for mass spectrometric analyses. ZAG coordinates have been deposited in the PDB (code 1zag). L.M.S. was supported by a grant from the U.S. Department of Defense Breast Cancer Research Program.

21 December 1998; accepted 18 February 1999

Acoel Flatworms: Earliest Extant Bilaterian Metazoans, Not Members of Platyhelminthes

Iñaki Ruiz-Trillo,[1] Marta Riutort,[1] D. Timothy J. Littlewood,[2] Elisabeth A. Herniou,[2] Jaume Baguñà[1]*

Because of their simple organization the Acoela have been considered to be either primitive bilaterians or descendants of coelomates through secondary loss of derived features. Sequence data of 18S ribosomal DNA genes from non–fast evolving species of acoels and other metazoans reveal that this group does not belong to the Platyhelminthes but represents the extant members of the earliest divergent Bilateria, an interpretation that is supported by recent studies on the embryonic cleavage pattern and nervous system of acoels. This study has implications for understanding the evolution of major body plans, and for perceptions of the Cambrian evolutionary explosion.

"Since the first Metazoa were almost certainly radial animals, the Bilateria must have sprung from a radial ancestor, and there must have been an alteration from radial to bilateral symmetry. This change constitutes a most difficult gap for phylogeneticists to bridge, and various highly speculative conjectures have been made" (*1*, p. 5). So began Libbie Hyman's discussion on the origin of bilaterian Metazoa, and despite a century of morphological studies and a decade of intensive molecular work, the nature of the simplest bilaterian animal remains elusive (*1, 2*). Paleontological and molecular data indicate that most bilaterian phyla appeared and diversified during the Cambrian explosion (*3, 4*). Three main clades emerged—

the Deuterostomia, the Ecdysozoa, and the Lophotrochozoa (*5*), although their branching order is unresolved. The acoel flatworms, traditionally classified as an order of the Platyhelminthes, are perhaps the simplest extant members of the Bilateria and have been viewed as either basal metazoans that evolved from ciliate protozoans ("syncytial or ciliate-acoel theory") (*6*) or a direct link between diploblasts and triploblasts ("planuloid-acoeloid theory") (*1, 7*). However, the lack of complexity has also been interpreted as a loss of derived features of more complex ancestors ("archicoelomate theory") (*8*).

The proposed metazoan phylogenetic trees that include acoels have shown them to branch after the diploblasts, indicating that they are considered primitive triploblastic animals (*9–11*). However, all 18*S* ribosomal DNAs (rDNAs) from acoels that have been sequenced so far show rates of nucleotide substitution that are three to five times the rates of most other Metazoa (*10*), resulting in the long-branch attraction effect in which rapidly evolving taxa cluster and branch together artifactually at the deepest base of the trees (*12*). We examined the relationship of the Acoela to other metazoan taxa by sequencing complete 18*S* rDNAs (*13*) from 18 acoel species (*14*). In addition, we sequenced the 18*S* rDNA of the catenulid *Suomina* sp. and the nemertodermatid *Meara* sp. as additional representatives of basal orders of Platyhelminthes thought to be closely related to acoels. The 18*S* ribosomal gene was chosen because of the large number of sequences available in the molecular data banks (GenBank and European Molecular Biology Laboratory) for representatives of the entire animal kingdom.

To avoid the long-branch effect, we broadly sampled the Acoela to find species that have normal rates of nucleotide substitution (non–fast-clock species). As representatives of most animal phyla a wide range of metazoan species were selected from the data banks (Table 1) and their sequences aligned and compared with those of acoels (*15*). A preliminary phylogenetic analysis (by the neighbor-joining method) showed that all 18 acoels form a very clear monophyletic group that branches at the base of the triploblasts. As expected (*10*), inclusion of the long-branch acoels leads to several inconsistencies in tree topology. Therefore, to select those taxa with uniform rates of change, we first performed a relative rate test (*16*) comparing all the species by pairs with the diploblast species as reference taxa. Because extremely long branches characterize most acoel species, only the four with shortest branches were included in the test. Only one acoel species (*Paratomella rubra*) passed the test, and one other (*Simplicomorpha gigantorhabditis*) came very close (Table 1). Although the latter was not included in subsequent analyses reported here, very similar results were obtained when both species or a single one (*Paratomella rubra*) was used. Of 74 bilaterian species tested (including the four acoels), 57 passed the test. Subsequent analyses were performed with only these 57 species that demonstrated uniform and comparable rates of evolution (representing 21 phyla) plus the four diploblasts representing three phyla. The second step in the analysis was to determine the phylogenetic content of the data resulting from this selection. Two tests were carried out. A plot of the observed (total, transitions or transversions) versus inferred number of substitutions (*4, 17*) showed that, although the curves tend to level off (Fig. 1A), they do not reach a plateau, meaning that the sequences studied are only moderately mutationally saturated. From a likelihood-mapping analysis (*18*) 81.5% of quartets had resolved phylogenies and only 10.7% of all quartet points were in the star-tree region (Fig. 1B), indicating that the rDNA data contain a reasonably high degree of phylogenetic information.

We next built a tree using maximum likelihood (*19*). The best tree that we found is shown in Fig. 2. In this tree, Deuterostomia, Ecdysozoa, and Lophotrochozoa (*5*) form monophyletic groups. Interestingly, the acoelomate and pseudocoelomate groups cluster at the base of the Ecdysozoa and Lophotrochozoa. Most importantly, the tree shows the acoels as the first offshoot after the diploblasts. However, the nemertodermatids, an order of Platyhelminthes usually classified as the sister group of the Acoela and forming the Acoelomorpha (*20, 21*), and here represented by the single species that passed the relative rate test, group within the bulk of the Platyhelminthes rather than with the acoels. On the other hand, both catenulids cluster at the base of the Platyhelminthes. All alternative hypotheses concerning the relationships between acoels and other platyhelminths (*20, 22–24*) and their position within the Bilateria (*10*) were also compared by the Kishino-Hasegawa test and all were significantly poorer

Table 1. List of species included in this study, GenBank accession numbers, and result of the relative rate test (rrt). The names of the 61 species finally selected for analysis are in bold. Ph., phylum; O., order; Cl., class.

Taxa	Species	Acc. number	rrt*	
			5%	1%
Deuterostomia				
Ph. Chordata	***Branchiostoma floridae***	M97571	0	0
	Lampetra aepyptera	M97573	0	0
	Xenopus laevis	X04025	0	0
	Mus musculus	X00686	0	0
Ph. Hemichordata	***Balanoglossus carnosus***	D14359	0	0
	Saccoglossus kowalewskii	L28054	0	0
Ph. Echinodermata	***Antedon serrata***	D14357	0	0
	Ophioplocus japonicus	D14361	0	0
Lophotrochozoa				
Ph. Mollusca	***Acanthopleura japonica***	X70210	0	0
	Lepidochitona corrugata	X91975	0	0
	Argopecten irradians	L11265	0	0
	Chlamys islandica	L11232	0	0
	Nerita albiulla	X91971	0	0
	Limicolaria hambeul	X60374	0	0
Ph. Annelida	***Eisenia foetida***	X79872	0	0
	***Enchytraeus* sp.**	U95948	0	0
	Hirudo medicinalis	Z83752	0	0
	Haemopsis sanguisua	X91401	0	0
	Lanice conchilega	X79873	0	0
	Nereis virens	Z83754	0	0
Ph. Nemertini	***Prostoma eilhardi***	U29494	0	0
	***Lineus* sp.**	X79878	0	0
Ph. Sipuncula	***Phascolosoma granulatum***	X79874	0	0
Ph. Brachiopoda	***Terebratalia transversa***	U12650	0	0
	Lingula lingua	X81631	0	0
Ph. Entoprocta	***Barentsia hildegardae***	AJ001734	0	0
Ph. Bryozoa	***Pedicellina cernua***	U36273	0	0
	Plumatella repens	U12649	0	0
Ph. Phoronida	***Phoronis vancouverensis***	U12648	0	0
Ph. Echiura	***Ochetostoma erythrogrammom***	X79875	0	0
Ph. Pogonophora	***Ridgeia piscesae***	X79877	0	0
	Siboglinum fiordicum	X79876	0	0
Ph. Gastrotricha	***Lepidodermella squammata***	U29198	0	0
	***Chaetonotus* sp.**	AJ001735	0	0

[1]Departament de Genètica, Facultat de Biologia, Universitat de Barcelona, Diagonal 645, 08028 Barcelona, Spain. [2]Department of Zoology, The Natural History Museum, Cromwell Road, London SW7 5BD, UK.

*To whom correspondence should be addressed. E-mail: bagunya@porthos.bio.ub.es

Table 1. *Continued*

Taxa	Species	Acc. number	rrt* 5%	rrt* 1%
Lophotrochozoa (continued)				
Ph. Platyhelminthes				
O. Acoela†	***Paratomella rubra*‡**	AF102892	0	0
	Simplicomorpha gigantorhabditis‡	AF102894	14	0
	Symsagittifera psammophila‡	AF102893	41	10
	Haplogonaria syltensis‡	AF102900	45	45
O. Tricladida	*Polycelis nigra*	AF013151	9	0
O. Polycladida	***Discocelis tigrina***	U70074	0	0
O. Lecithoepitheliata	***Geocentrophora* sp.**	U70080	0	0
O. Macrostomida	***Macrostomum tuba***	U70081	0	0
	Microstomum lineare	U70083	0	0
O. Proseriata	***Monocelis lineata***	U45961	0	0
O. Nemertodermatida	***Nemertinoides elongatus***	U70084	0	0
	Meara sp.‡	AF051328	32	5
O. Catenulida	***Stenostomum leucops***	U70085	0	0
	***Suomina* sp.‡**	AJ012532	0	0
Cl. Cestoda	*Grillotia erinaceus*	AJ228781	13	0
Cl. Trematoda	***Schistosoma mansoni***	M62652	1	0
	Fasciolopsis bushi	L06668	1	0
Cl. Monogenea	*Neomicrocotyle pacifica*	AJ228787	9	0
Ecdysozoa				
Ph. Tardigrada	***Macrobiotus hufelandi***	X81442	0	0
Ph. Arthropoda	***Odiellus troguloides***	X81441	0	0
	***Aphonopelma* sp.**	X13457	0	0
	Berndtia purpurea	L26511	0	0
	Panulirus argus	U19182	0	0
	Tenebrio molitor	X07801	0	0
	Polistes dominulus	X77785	0	0
	Scolopendra cingulata	U29493	0	0
Ph. Priapulida	***Priapulus caudatus***	X87984	0	0
Ph. Kinorhyncha	***Pycnophyes hielensis***	U67997	0	0
Ph. Nematomorpha	***Gordius aquaticus***	X87985	0	0
Ph. Nematoda	*Trichinella spiralis*	U60231	10	0
	Plectus sp.	U61761	34	8
	Zeldia punctata	U61760	43	14
Other phyla				
Ph. Chaetognatha	*Paraspadella gotoi*	D14362	44	19
Ph. Mesozoa	*Dicyema* sp.	X97157	45	28
	Rhopalura ophiocomae	X97158	29	1
Ph. Gnathostomulida	*Gnathostomula paradoxa*	Z81325	45	32
Ph. Rotifera	*Philodina acuticornis*	U91281	45	44
	Brachionus plicatilis	U49911	0	0
Ph. Acanthocephala	*Moliniformis moliniformis*	Z19562	10	0
	Neoechynorhynchus pseudemydis	U41400	25	0
Diploblasts				
Ph. Placozoa	***Trichoplax adhaerens***	L10828		
Ph. Porifera	***Scypha ciliata***	L10827		
Ph. Cnidaria	***Anemonia sulcata***	X53498		
	Tripedalia cystophora	L10829		

*Figures indicate the number of cases in which the rate of nucleotide substitutions of each species was significantly different (at 5% and at 1% levels) when compared by pairs with a set of 45 species with a uniform rate of substitution. Diploblasts served as reference species. For further details, see (*16*). The complete matrix with all the comparisons is available at ftp://porthos.bio.ub.es/pub/incoming/phylogeny/rrt.xls †A total of 18 species of acoels were sequenced, though only the four earliest branching taxa within that group were used in the metazoan-wide analysis. For the rest of acoel sequences, see (*14*). ‡New sequences reported in this paper.

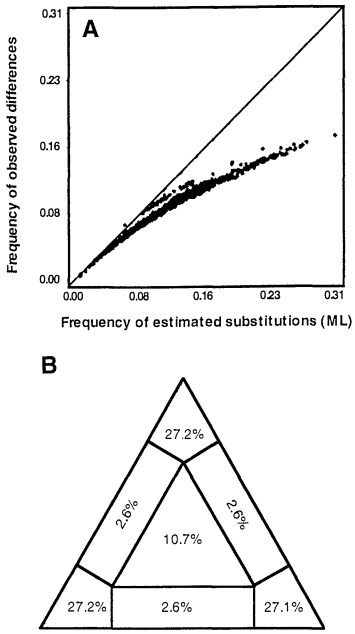

Fig. 1. Phylogenetic content of the data. (**A**) Substitution saturation curve. The *y* axis shows the frequency of observed differences between pairs of species sequences determined with MUST (*4, 17*), and the *x* axis shows the inferred distance between the same two sequences determined by maximum likelihood (ML) with PUZZLE v. 4.0 (*38*). Each dot thus defines the observed compared with the inferred number of substitutions for a given pair of sequences. The resulting curve lies between the diagonal line (no saturation) and a horizontal plateau line (full saturation), which means that the data set is only moderately saturated [for further information see (*4, 17*)]. (**B**) Likelihood mapping analysis (*18*) of the data set, represented as a triangle. Values at the corners indicate the percentages of well-resolved phylogenies for all possible quartets (*18*), and values at the central and lateral regions are percentages of unresolved phylogenies. The cumulatively high percentage (81.5%) from the corner values indicates the data set is phylogenetically informative.

than the phylogeny obtained originally. The robustness of the internal branch separating acoels from the rest of bilaterians was further evaluated by the four-cluster likelihood mapping method (*25*) and resulted in 100% support for this branch.

Because the position of the acoels might be due to the most variable sites of the alignment, we removed them from the whole data set (*26*); the acoels still appeared at the base of the trees, although the phylogenetic signal within the triploblasts almost faded away. Alternatively, the sequence regions that show the highest variation among acoels might represent noisy data that separate them from the rest of the Bilateria. To test this idea, we aligned the 18 acoel sequences, found their most variable positions, and removed the latter from the 61-species alignment (*27*). Again, this resulted in the acoels on a shorter branch at the base of the bilaterian tree (the three trees obtained in both tests are available as supplementary material at www.sciencemag.org/feature/data/986597.shl). Finally, because some important phyla such as Chaetognatha, Acanthocephala, Gnathostomulida, Mesozoa, and Nematoda did not pass the relative rate test and were not included in the maximum-likelihood analyses, the four-cluster likelihood mapping was used again to test the position of these groups against acoels and the rest of the triploblasts. In all cases, acoels and diploblasts cluster together (Table 2). Importantly, of all the phyla tested, some of those previously proposed as "primitive" bilaterians (Mesozoa, Nematoda, and Gnathostomulida), always cluster with the triploblasts.

Our analyses clearly indicate that acoels are not members of the phylum Platyhelminthes, but occupy a key position in the Metazoan tree of life, most likely as the earliest branch within the bilaterian clade that left extant descendants. The monophyly of Platyhelminthes has been criticized (*23, 28, 29*) because of the weakness

Table 2. Four-cluster likelihood mappings to test acoel position against fast-clock phyla. Four-cluster likelihood mappings (*18*) were performed arranging species into three groups: diploblasts (D), acoels (A), triploblasts (T), and a fourth group (X) taken from each of the phyla to be tested. If the phylum under test is more basal than the acoels, it should cluster with high support with the diploblasts. Conversely, if acoels are more basal the phylum under test should cluster with the triploblasts. Results show that acoels cluster more closely to the diploblasts than all other triploblasts.

Fast-clock phyla (X)	Bifurcating tree			Intermediate regions	Star tree
	D A \ T X / D T	A D \ X X / A T			
Acanthocephala	98.2%	0%	0%	1.8%	0%
Chaetognatha	98.7%	0%	0%	1.3%	0%
Gnathostomulida	75.4%	15.2%	0%	9.4%	0%
Mesozoa	93.1%	0%	0%	5.1%	1.8%
Nematoda	99.7%	0%	0%	0.3%	0%

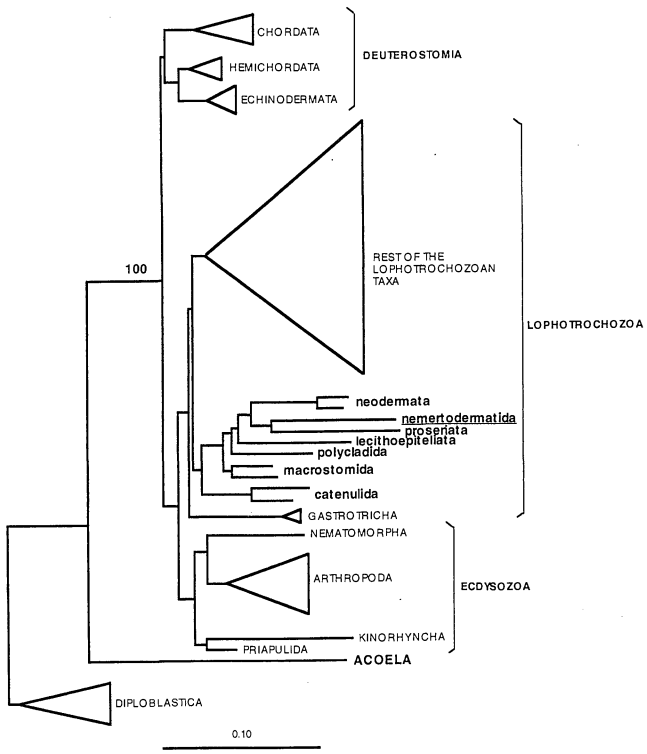

Fig. 2. Diagrammatic representation of the best 18*S* rDNA-based maximum-likelihood tree of 61 metazoan species (bold names are in Table 1) with homogeneous rates of nucleotide substitution. The final matrix included 1181 sites (584 variable and 383 informative under parsimony); log ln = 11,862. The number 100 on the branch separating acoels from the rest of triploblasts represents the percentage of support to that branch obtained by the four-cluster likelihood mapping (*25*). The tree was obtained with fast DNAml (*19*). It illustrates the relationships of the Acoela (bold, upper case) and the rest of the Platyhelminthes (bold, lower case) to the rest of the Metazoa. The general topology of the tree defines three main bilaterian phylogenetic groups: Deuterostomia, Lophotrochozoa (including Platyhelminthes and Gastrotricha as basal phyla), and Ecdysozoa (with Priapulida and Kinorhynchia as basal phyla). The position of the Acoela renders the Platyhelminthes polyphyletic, whereas the Nemertodermatida (underlined) appears buried within the bulk of Platyhelminthes. For taxa and species names, see Table 1, the complete tree with all the species names is available in the supplementary material at www.sciencemag.org/feature/data/986597.shl

of the synapomorphies on which it is based (*22, 24*): multiciliation of epidermal cells, the biciliary condition of the protonephridia, and the lack of mitosis in somatic cells. In contrast, the Acoela have a characteristic set of well-defined apomorphies: a network of ciliary roots of epidermal cells, tips of the cilia with a distinct step, lack of extracellular matrix, absence of protonephridia, and, most importantly, the duet spiral cleavage. The first three features are usually considered to be derived (*22, 24*); the 18*S* molecular data, however, suggest a different interpretation for the other two. The lack of protonephridia in acoels may be a plesiomorphic feature (*29*). The Acoela exhibit duet spiral cleavage, in contrast to the quartet pattern that characterizes the Spiralia and some turbellarian Platyhelminthes. However, acoel cleavage is actually more bilateral than spiral (*30*), suggesting that duet cleavage and typical quartet cleavage are not related. Moreover, all spiralian embryos have both ecto- and endomesoderm and exhibit determinative development, whereas acoel embryos generate only endomesoderm (*30*) and are highly regulative (*31*); the latter two features are considered to be ancestral. Most diploblastic and several triploblastic phyla exhibit a radial cleavage pattern; thus, it is more parsimonious to assume that the first bilaterian also had radial cleavage (*32*). This evidence supports our proposed phylogenetic tree in which the acoels branch before the Cambrian radiation from unknown bilaterian ancestors with radial cleavage and suggests that duet cleavage and quartet spiral cleavage arose independently from an ancestral radial pattern. The structure of the nervous system also indicates that the acoels are not related to the other platyhelminths. Most Platyhelminthes have a bilobed brain with neuropile surrounded by nerve cells and two main longitudinal nerve cords with commisures making an orthogon (*33*). In contrast, the nervous system of acoels comprises a simple brain formed by clusters of nerve cells that lack a neuropile, and a variable number of longitudinal nerve cords that do not make an orthogon (*34*).

The 18*S* rDNA sequences, embryonic cleavage patterns and mesodermal origins (*30*), and nervous system structure data (*34*) support the position of the Acoela as the earliest branching Bilateria (Fig. 2) and the polyphyly of the Platyhelminthes. This argues for an extended period before the Cambrian within which different bilaterian lineages may have originated, with the acoels being the descendants of one of these lineages. This interpretation is supported by recent data on protein sequence divergence (*35*). Direct development, which characterizes all extant acoels, as opposed to the biphasic life cycle with a larval stage and a benthic adult (*36*), probably represents the ancestral bilaterian condition [see (*37*), for a recent discussion]. Our findings suggest that the Acoela (or Acoelomorpha if the Nemertodermatida are shown to remain as their sister group) should be placed in their own phylum.

References and Notes

1. L. H. Hyman, *The Invertebrates. II. Platyhelminthes and Rhynchocoela. The Acoelomate Bilateria* (McGraw-Hill, New York, 1951).
2. R. C. Brusca and G. J. Brusca, *The Invertebrates* (Sinauer, Sunderland, MA, 1990); C. Nielsen, *Animal Evolution, Interrelationships of the Living Phyla* (Oxford Univ. Press, Oxford, 1995).
3. S. Conway-Morris, *Nature* **361**, 219 (1993); R. A. Raff, C. R. Marshall, J. M. Turbeville, *Annu. Rev. Ecol. Syst.* **25**, 351 (1994); S. Conway-Morris, *The Crucible of Creation* (Oxford Univ. Press, Oxford, 1998).
4. H. Philippe, A. Chenuil, A. Adoutte, *Development* **1994** (suppl.), 15 (1994).
5. A. M. A. Aguinaldo *et al.*, *Nature* **387**, 489 (1997).
6. J. Hadzi, *The Evolution of the Metazoa* (Macmillan, New York, 1963)
7. L. V. von Salvini-Plawen, *Z. Zool. Syst. Evolutionsforsch.* **16**, 40 (1978).
8. P. Ax, in *The Lower Metazoa*, E. C. Dougherty, Ed. (Univ. of California Press, Berkeley, CA, 1963), pp. 191–224; R. Siewing, *Zool. Jahrb. Anat.* **103**, 439 (1980); R. M. Rieger, in *The Origins and Relationships of Lower Invertebrates*, S. Conway-Morris *et al.*, Eds. (Clarendon, Oxford, 1985), pp. 101–122; J. P. S. Smith and S. Tyler, in *ibid.*, pp. 123–142.
9. T. Katayama, M. Yamamoto, H. Wada, N. Satoh, *Zool. Sci.* **10**, 529 (1993); B. Winnepenninckx, T. Backeljau, R. De Wachter, *Mol. Biol. Evol.* **12**, 641 (1995); J. Zrzavy, S. Mihulka, P. Kepka, A. Bezdek, D. Tietz, *Cladistics* **14**, 249 (1998).

10. S. Carranza, J. Baguñà, M. Riutort, *Mol. Biol. Evol.* **14**, 485 (1997).
11. D. T. J. Littlewood, K. Rohde, K. A. Clough, *Biol. J. Linn. Soc.* **66**, 75 (1999).
12. J. Felsenstein, *Syst. Zool.* **27**, 401 (1978); G. J. Olsen, *Cold Spring Harb. Symp. Quant. Biol.* **LII**, 825 (1987).
13. The 18*S* rDNA was amplified and sequenced from high molecular weight genomic DNA as described [(*11*); S. Carranza, G. Giribet, C. Ribera, J. Baguñà, M. Riutort, *Mol. Biol. Evol.* **13**, 824 (1996)].
14. Sequences have been deposited in the GenBank under accession numbers AF102892 to AF102900 and AJ012522 to AJ012530.
15. Sequences were aligned by eye on the basis of the secondary structure model [R. R. Gutell, B. Weibser, C. R. Woese, H. F. Noller, *Prog. Nucleic Acid Res. Mol. Biol.* **32**, 155 (1985)] with GDE v.2.2. Positions that could not be unambiguously aligned were removed from the alignment. The final matrix contained 1181 sites (including 584 variable, 383 informative under parsimony); the full final alignment is deposited under accession number ds37667.dat and is available at ftp://FTP.EBI.AC.UK under directory pub/databases/embl/align.
16. The relative rate test [A. C. Wilson, S. S. Carlson, T. J. White, *Annu. Rev. Biochem* **46**, 573 (1977)] compares genetic distances between each of two species and a reference outgroup. We performed the test according to W. H. Li and M. Tanimura, *Nature* **326**, 93 (1987). A first set of 45 bilaterian species (deuterostomes; ecdysozoans, with the exception of Nematoda; and lophotrochozoans, with the exception of Platyhelminthes) with slow and uniform rates of nucleotide substitution, as reflected in their similarly short branch lengths in most published phylogenetic trees, were selected and compared by pairs with diploblasts as reference outgroups. As expected, all were found to have uniform relative rates of nucleotide substitution. Then, a second set of 29 bilaterian species from phyla known to have rates higher than the first set (Platyhelminthes including acoels, Nematoda, Chaetognata, Mesozoa, Gnathostomulida, Rotifera, and Acanthocephala) were compared with each of the species of the first group (45 species) with diploblasts as reference. The results are expressed in Table 1 as the number of cases in which each species has a rate significantly different from those of the first group at the 1% and at the 5% levels.
17. H. Philippe, *Nucleic Acid Res.* **21**, 5264 (1993). The analysis shows the relation between the number of changes that have occurred (as deduced from the tree), and the number of changes that can be calculated directly from the sequence alignment. When the sequences are saturated, it is expected that although the number of inferred changes still increases (*x* axis), they are no longer detected as observed differences (leveling along the *y* axis), so the line defined by the points levels off from the diagonal in the graph and becomes horizontal.
18. The likelihood mapping analysis [(*38*); K. Strimmer and A. von Haeseler, *Proc. Natl. Acad. Sci. U.S.A.* **94**, 6815 (1997)] is a graphical method to visualize the phylogenetic content of a set of aligned sequences. Likelihoods of all quartet trees for each subset of four species are mapped on a triangle, and the triangle is partitioned in different regions. The central region represents starlike evolution, the three corners represent well-resolved phylogeny, and three intermediate regions between corners represent where it is difficult to distinguish between two of the three trees. The resulting distribution of points indicates whether or not the data are suitable for a phylogenetic reconstruction: the phylogenetic information in the data is higher when the value in the central region is smaller.
19. Tree reconstruction was performed by maximum likelihood with both fastDNAml v.1.1.1.a [G. J. Olsen, H. Matsuda, R. Hangstrom, R. Overbeek, *Comput. Appl. Biosci.* **10**, 41 (1994)] and PUZZLE v. 4.0 (*38*) programs. We built an initial tree with fastDNAML using global rearrangements and jumble options and subjected it to the Kishino-Hasegawa test against alternative topologies using PUZZLE [HKY model of substitution; M. Hasegawa, H. Kishino, K. Yano, *J. Mol. Evol.* **22**, 160 (1985)]. The parameters for rate heterogeneity among sites were inferred from the data set. The best tree found was resubmitted to a global rearrangement search with fastDNAML, taking into account among-site rate variation by using the rate and category parameters calculated by PUZZLE.
20. T. G. Karling, in *Biology of the Turbellaria*, N. W. Riser and M. P. Morse, Eds. (McGraw-Hill, New York, 1974), pp. 1–16.
21. P. Ax, *The Phylogenetic System. The Systematization of Organisms on the Basis of Their Phylogenesis* (Wiley, Chichester, UK, 1987).
22. U. Ehlers, *Das Phylogenetische System der Plathelminthes* (Fischer, Stuttgart, 1985).
23. J. P. S. Smith, S. Tyler, R. M. Rieger, *Hydrobiologia* **132**, 13 (1986).
24. P. Ax, *Multicellular Animals, A New Approach to the Phylogenetic Order in Nature* (Springer-Verlag, Berlin, 1996).
25. To analyze the support for internal branches in a tree without having to compute the overall tree, we performed four-cluster likelihood mapping using PUZZLE 4.0 (*38*). Every internal branch in a completely resolved tree defines up to four clusters of sequences. These four clusters can be defined in the data file, and the program will build a quartet tree for each of all possible combinations of four species, always taking one from each group. The result is represented on a triangle (*18*). The distribution of points within this triangle indicates the level of support for the internal branch under analysis.
26. We used PUZZLE 4.0 (*38*) to find the parameters for among-site rate heterogeneity. Resulting data were divided into eight categories, each with an assigned rate value (from constant to diverse values of variability). In two successive analyses we eliminated from the 61 species alignment those positions that were more variable (category 8) and also the sites with the two most variable categories (7 and 8). From these new data sets trees were reconstructed with fastDNAML (*19*).
27. An alignment including only the 18 acoel sequences was used to find their most variable positions and those sites [category 8, see (*26*)] were removed from the 61 species alignment. From this new data set trees were reconstructed with fastDNAML (*19*).
28. R. M. Rieger, S. Tyler, J. P. S. Smith, G. E. Rieger, in *Microscopic Anatomy of Invertebrates*, vol. 3, *Platyhelminthes and Nemertinea*, F. W. Harrison and B. J. Bogitsh, Eds. (Wiley-Liss, New York, 1991), pp. 7–140.
29. G. Haszprunar, *J. Zool. Syst. Evol. Res.* **34**, 41 (1996).
30. B. C. Boyer and J. Q. Henry, *Am. Zool.* **38**, 621 (1998); J. J. Henry, M. Q. Martindale, B. C. Boyer, personal communication.
31. B. C. Boyer, *J. Exp. Zool.* **176**, 96 (1971).
32. J. W. Valentine, *Proc. Natl. Acad. Sci. U.S.A.* **94**, 8001 (1997).
33. E. Reisinger, *Z. Zool. Syst. Evolutionsforsch.* **10**, 1 (1972).
34. O. I. Raikova, M. Reuter, E. A. Kotikova, M. K. S. Gustafsson, *Zoomorphology* **118**, 69 (1998); M. Reuter, O. I. Raikova, M. K. S. Gustafsson, *Tissue Cell* **30**, 57 (1998).
35. G. A. Wray, J. S. Levinton, L. H. Shapiro, *Science* **274**, 568 (1996); F. J. Ayala, A. Rzhetsky, F. J. Ayala, *Proc. Natl. Acad. Sci. U.S.A.* **95**, 606 (1998); L. Bromham, A. Rambaut, R. Fortey, A. Cooper, D. Penny, *ibid.* **95**, 12386 (1998).
36. G. Jägersten, *Evolution of the Metazoan Life Cycle: A Comprehensive Theory* (Academic Press, London, 1972); R. M. Rieger, *Am. Zool.* **34**, 484 (1994).
37. S. Conway-Morris, *Bioessays* **20**, 676 (1998).
38. K. Strimmer and A. von Haeseler, *Mol. Biol. Evol.* **13**, 964 (1996).

39. We thank M. Martindale, J. Henry, and B. Boyer for their insightful comments and sharing of previous results; S. Carranza for his help in the first stages of this work; A. Adoutte, J. McInerney, G. Olsen, H. Philippe, and K. Strimmer for methodological advice; and R. Bray, L. Colin, M. Dawson, A. Faubel, K. Lundin, L. Martin, O. Raikova, R. Rieger, K. Rohde, J. P. S. Smith, and S. Tyler who provided material for this study. I.R.-T., M.R., and J.B. were supported by CIRIT (Generalitat de Catalunya) grants 1995SGR-00574 and 1997SGR-00057. D.T.J.L. and E.A.H. were funded by a Wellcome Trust Senior Research Fellowship to D.T.J.L. (043965/Z/95/Z). J.B. and D.T.J.L. shared the grant HB1996-0034 from the British-Spanish Joint Research Programme (Acciones Integradas).

18 November 1998; accepted 9 February 1999

Rapid Dendritic Morphogenesis in CA1 Hippocampal Dendrites Induced by Synaptic Activity

M. Maletic-Savatic, R. Malinow, K. Svoboda

Activity shapes the structure of neurons and their circuits. Two-photon imaging of CA1 neurons expressing enhanced green fluorescent protein in developing hippocampal slices from rat brains was used to characterize dendritic morphogenesis in response to synaptic activity. High-frequency focal synaptic stimulation induced a period (longer than 30 minutes) of enhanced growth of small filopodia-like protrusions (typically less than 5 micrometers long). Synaptically evoked growth was long-lasting and localized to dendritic regions close (less than 50 micrometers) to the stimulating electrode and was prevented by blockade of *N*-methyl-D-aspartate receptors. Thus, synaptic activation can produce rapid input-specific changes in dendritic structure. Such persistent structural changes could contribute to the development of neural circuitry.

Coordinated patterns of activity help to organize neural circuits throughout the brain (*1*). In particular, activity shapes the structure of sensory maps (*2*) and individual neurons (*3*) through *N*-methyl-D-aspartate (NMDA) receptor–dependent processes, which suggests that synapse-specific associative changes are involved. Relatively little is known about the role of activity in the development of dendritic morphology. A number of studies have addressed whether long-term potentiation (LTP) produces postsynaptic structural changes. Using electron microscopy (EM) analysis of fixed

Cold Spring Harbor Laboratory, Cold Spring Harbor, NY 11724, USA.